A&A, 691, A46 (2024)
https://doi.org/10.1051/0004-6361/202451076

Astronomy & Astrophysics

A census of the Sun's ancestors and their contributions to the Solar System chemical composition

F. Fiore[1,⋆], F. Matteucci[1,2,3], E. Spitoni[2,⋆], M. Molero[4,2], P. Salucci[5,3], D. Romano[6], and A. Vasini[1,2]

[1] Dipartimento di Fisica, Sezione di Astronomia, Università di Trieste, Via G. B. Tiepolo 11, 34143 Trieste, Italy
[2] I.N.A.F. Osservatorio Astronomico di Trieste, via G.B. Tiepolo 11, 34131 Trieste, Italy
[3] I.N.F.N. Sezione di Trieste, via Valerio 2, 34134 Trieste, Italy
[4] Institut für Kernphysik, Technische Universität Darmstadt, Schlossgartenstr. 2, Darmstadt 64289, Germany
[5] SISSA-International School for Advanced Studies, Via Bonomea 265, 34136 Trieste, Italy
[6] INAF, Osservatorio di Astrofisica e Scienza dello Spazio, Via Gobetti 93/3, 40129 Bologna, Italy

Received 12 June 2024 / Accepted 23 September 2024

ABSTRACT

In this work, we compute the rates and numbers of different types of stars and phenomena (supernovae, novae, white dwarfs, merging neutron stars, black holes) that contributed to the chemical composition of the Solar System. During the Big Bang, only light elements formed, while all the heavy ones, from carbon to uranium and beyond, have since been created inside stars. Stars die and release the newly formed elements into the interstellar gas. This process is called 'chemical evolution'. In particular, we analyse the death rates of stars of all masses, whether they die quiescently or explosively. These rates and total star numbers are computed in the context of a revised version of the two-infall model for the chemical evolution of the Milky Way, which reproduces the observed abundance patterns of several chemical species, the global solar metallicity, and the current gas, stellar, and total surface mass densities relatively well. We also compute the total number of stars ever born and still alive as well as the number of stars born up to the formation of the Solar System with mass and metallicity like those of the Sun. This latter number accounts for all the possible existing Solar systems that can host life in the solar vicinity. We conclude that, among all the stars (from 0.8 to 100 $M_\odot$) that were born and died from the Big Bang up until the Solar System formation epoch and that contributed to its chemical composition, 93.00% were stars that died as single white dwarfs (without interacting significantly with a companion star) and originated in the mass range of 0.8–8 $M_\odot$, while 5.24% were neutron stars and 0.73% were black holes, both originating from core-collapse supernovae (M > 8 $M_\odot$); 0.64% were Type Ia supernovae and 0.40% were nova systems, both originating from the same mass range as the white dwarfs. The number of stars similar to the Sun born from the Big Bang up until the formation of the Solar System, with metallicity in the range 12+log(Fe/H)= 7.50 ± 0.04 dex, is ~$31\cdot 10^7$, and in particular our Sun is the ~$2.61\cdot 10^7$-th star of this kind.

Key words. ISM: abundances – Galaxy: abundances – Galaxy: disk – Galaxy: evolution – solar neighborhood

1. Introduction

Stars are born, they live, and they die. During their lives they produce new chemical elements starting from H and He, forming all the elements from carbon to uranium and beyond. Stars then eject these newly formed elements both by stellar winds and through supernova (SN) explosions, thus increasing their abundance in the interstellar medium (ISM). This process is known as galactic chemical evolution and is responsible for the chemical composition of the Solar System, which was born 4.6 Gyr ago (e.g. Bouvier & Wadhwa 2010). In order to study chemical evolution, we need to build detailed models that include several physical ingredients, including star formation rate (SFR), initial mass function (IMF), stellar nucleosynthesis, and gas flows. There are many such models in the literature, but very few are detailed enough to follow the evolution of many chemical species and to take into account all the necessary stellar sources that we are listing below. In particular, massive stars ($M > 8\,M_\odot$) ending their lives as core-collapse supernovae (CC-SNe) are responsible for the production of α-elements (e.g. O, Ne, Mg, Ca, Si, and Ti) and r-process elements (which are formed also by means of merging neutron stars), while low- and intermediate-mass stars ($0.8 \leq M/M_\odot \leq 8$) produce C, N, and heavy s-process elements (e.g. Ba, Y, and La). Supernovae Type Ia (exploding white dwarfs in binary systems) are responsible for the production of most of the Fe in the Universe and novae, also originating from white dwarfs (WDs) in binary systems, are not negligible producers of CNO isotopes as well as ^{7}Li. These models relax the instantaneous recycling approximation and compute – in detail – the rates of SNe of all types, novae, and merging neutron stars. Taking into account the lifetimes of these different stellar types is fundamental in order to correctly predict the abundances of the elements and their ratios. Clearly, the stellar yields as functions of stellar mass and metallicity represent one of the most important ingredients of such models, together with the stellar birthrate function (star formation rate and initial mass function) and possible gas flows (see Matteucci 2021 for a review).

In this paper, we focus on the Milky Way (MW) and, in particular, on the chemical evolution of the solar neighbourhood. Our main goal is to compute how many stars of different masses have contributed to building the chemical composition of the Solar System. In particular, we analyse the contributions of low- and intermediate-mass stars dying as WDs, CC-SNe, and merging neutron stars (MNSs). Moreover, we compute the number of black holes that have been created up until the birth of the Solar System. To this end, we adopt a detailed chemical

⋆ Corresponding author; emanuele.spitoni@inaf.it, FRANCESCA.FIORE2@studenti.units.it

evolution model that follows the evolution of several chemical species, for a total of 43 elements from H to Pb. The adopted model derives from the two-infall model originally developed by Chiappini et al. (1997) (see also Matteucci et al. 2014; Romano et al. 2019). Here, we use the revised version of Molero et al. (2023) (see Spitoni et al. 2019, 2020, 2021; Palla et al. 2020), focusing our study on the solar vicinity.

The paper is organised as follows: in Section 2 we present the adopted chemical evolution model; in particular, we describe the prescriptions we assume for the basic equations of chemical evolution, stellar initial mass function, star formation rate, stellar yields, and gas flows. In Sect. 3 we present the model results relative to the [α/Fe] versus [Fe/H] trends (where α = O, Mg, Si, Ca). The plot of the ratio between α-elements (α = O, Mg, Si, Ca) and Fe can be used as a cosmic clock thanks to the different timescales of production of αs and Fe (time-delay model, Tinsley 1979; Matteucci 2012), and provides information on the star formation history of the Galaxy. In the same section we provide the rates and numbers of SNe, WDs, novae, merging neutron stars, and black holes that occurred in the solar neighbourhood region until the formation of the Solar System. Additionally, we provide the different contributions of stars to the chemical composition of the Solar System. In Sect. 4 we show the results obtained for the number of stars born roughly 4.6 ± 0.1 Gyr ago with the same characteristics as the Sun: this is to obtain a rough estimation of the number of planetary systems similar to ours that might have formed in the Galaxy. Finally, in Sect. 5 we discuss our results and draw some conclusions.

2. Chemical evolution: The two-infall model

In order to discuss how different types of stars contribute to the chemical composition of the Solar System, it is important to describe the original two-infall model (Chiappini et al. 1997), and the revised version by Molero et al. (2023) (see also Spitoni et al. 2019, 2021, 2024; Palla et al. 2020), which we use in this paper. The two-infall model suggests that the MW formed in two main gas-infall events. According to the original model, the first event should have formed the in situ (inner) Galactic halo and the thick disc, while the second infall event should have formed the thin disc.

The delayed two-infall model adopted here is a variation of the classical two-infall model of Chiappini et al. (1997) developed to fit the dichotomy in the α-element abundances observed between the thick and thin disc stars not only in the solar vicinity (Gratton et al. 1996; Fuhrmann 1998; Hayden et al. 2014; Recio-Blanco et al. 2014, 2023; Mikolaitis et al. 2017) but also at different Galactocentric distances (e.g. Hayden et al. 2015). The model assumes that the first gas-infall event formed the thick disc, whereas the second infall event, delayed by ∼3 Gyr, formed the thin disc. It must be noted that the two-infall model adopted here is not designed to distinguish between the thick and thin disc populations geometrically or kinematically (see Kawata & Chiappini 2016). The first gas-infall event lasts about $\tau_1 \simeq 1$ Gyr, while for the second event, an inside-out scenario (see e.g., Matteucci & Francois 1989; Romano et al. 2000; Chiappini et al. 2001) of Galaxy formation is assumed, namely the timescale of formation of the various regions of the thin disc by gas infall increases with Galactocentric distance. It should be noted that the two main episodes described by the two-infall model are sequential in time but are completely independent. In the original model of Chiappini et al. (1997), a threshold gas density for star formation was assumed, which naturally produces a gap in the star formation between the end of the thick disc phase and the beginning of the thin disc phase, and therefore a dichotomy in the [α/Fe] versus [Fe/H] plane. However, even without the assumption of a gas threshold, the double-infall assumption creates a dichotomy by itself, which, though less pronounced, is sufficient to reproduce the data (see Spitoni et al. 2019).

2.1. The basic equations of chemical evolution

The basic equations that describe the evolution of the fraction of gas mass in the form of a generic chemical element i, G_i, in the solar vicinity are

$$\dot{G}_i(R,t) = -\psi(R,t)X_i(R,t) + \dot{G}_{i,inf}(R,t) + \dot{E}_i(R,t), \quad (1)$$

where X_i is the abundance of the analysed element in terms of mass, $\psi(t)$ is the SFR, $\dot{G}_{i,inf}(R,t)$ is the gas-infall rate, and $\dot{E}_i(R,t)$ is the rate of variation of the returned mass in the form of the chemical species i, both newly formed and restored unprocessed. This last term contains all the stellar nucleosynthesis and stellar lifetime prescriptions.

2.2. Star formation rate

The quantity we are interested in here is the so-called stellar birthrate function, which is the number of stars with mass dm that are formed in the time interval dt. It is factorised as the product of the SFR depending only on the time t, and the IMF, here assumed to be independent of time and being only a function of the mass m.

For the SFR, here we adopt the Schmidt-Kennicutt law as a parametrization (Schmidt 1959; Kennicutt 1998), according to which the SFR is proportional to the kth power of the surface gas density. The SFR can then be written as

$$\psi(t) \propto \nu\sigma^k_{gas}(t), \quad (2)$$

where ν is the efficiency of star formation, namely the SFR per unit mass of gas, and is expressed in Gyr^{-1}. For the halo-thick disc phase ν= 2 Gyr^{-1}, whereas for the thin disc ν is a function of the Galactocentric distance R_{GC}, with ν (R$_{GC}$=8 kpc) $\simeq$ 1 Gyr^{-1}, as in Molero et al. (2023) and Palla et al. (2020). It is important to highlight that gas temperature, viscosity, and magnetic fields are ignored in this empirical law even if they are expected to impact the SFRs of galaxies. Nevertheless, ignoring these parameters is a common choice for the SFR in most galaxy evolution models.

In the scenario described by the original two-infall model, there was supposed to be a gas threshold in the star formation. This created a stop in the star formation process between the formation of the thick and the thin disc. Here, we relax the assumption of a threshold in the gas density and the gap in the star formation is naturally created between the formation of the two discs, because, given the longer delay between the two infall episodes, the SFR becomes so small that a negligible number of stars is born in that time interval.

In this context, we can make an additional distinction between the phases described by the two-infall model based on the stars that were present and dominating in each phase. During the thick disc formation, the most important contribution was from CC-SNe, which are identified as Type II, Ib, and Ic SNe, while Type Ia SNe started making a substantial contribution only after a time delay (see Matteucci 2021). This important difference significantly impacts the production of chemical elements and Galaxy composition, and the resultant scenario is known as the time-delay model (Tinsley 1979; Matteucci 2012, 2021).

2.3. Initial mass function

The second ingredient in the stellar birthrate function is the IMF, which gives the distribution of stellar masses at birth and is commonly parameterised as a power law. To measure the IMF, it is necessary to count the stars as functions of their magnitude, and so nowadays we can only do that for the solar region of the MW. We use the IMF proposed by Kroupa et al. (1993), which in chemical evolution is often the one that provides the best agreement with observations (see Romano et al. 2005 for a discussion). It is a three-slope IMF, with the following expression:

$$\phi(m) = C \begin{cases} m^{-(1+0.3)} & \text{if } m \leq 0.5\ M_{\odot} \\ m^{-(1+1.2)} & \text{if } 0.5 < m/M_{\odot} < 1.0 \\ m^{-(1+1.7)} & \text{if } m > 1.0\ M_{\odot}, \end{cases} \quad (3)$$

with C being the normalisation constant derived by imposing that:

$$1 = \int_{0.1}^{100} m\varphi(m)\,\mathrm{d}m, \quad (4)$$

where $\varphi(m)$ is the IMF in number.

2.4. Gas infall

In the case of gas infall, the gas is often assumed to have a primordial composition, namely with zero metal content. Since pristine gas is enriched only in light elements such as H, He and a small part of Li and Be, the effect of the infall is that of diluting the metal content inside the Galaxy. In this work, different gas flows than the infall one (such as Galactic winds and/or Galactic fountains) are not included. In particular, Galactic fountains, which can occur in disc galaxies, have been proven not to impact in a significant manner the chemical evolution of the disc (see Melioli et al. 2009; Spitoni et al. 2009).

In the context of the delayed two-infall model (Molero et al. 2023) adopted here, the accretion term is computed as:

$$\dot{G}_{i,inf}(R,t) = AX_{i,inf}e^{-\frac{t}{\tau_1}} + \theta(t - t_{max})BX_{i,inf}e^{\frac{-(t-t_{max})}{\tau_2}}, \quad (5)$$

where $X_{i,inf}$ is the composition of the infalling gas, here assumed to be primordial for both infall events. τ_1=1 and τ_2=7 Gyr are the infall timescales for the first and the second accretion event, respectively, and $t_{max} \simeq 3.25$ Gyr is the time for the maximum infall on the thin disc and corresponds to the start of the second infall episode. The parameters A and B are fixed to reproduce the surface mass density of the MW disc at the present time in the solar neighbourhood. In particular, A reproduces the total surface mass density of the thick disc at the present time (12 $M_{\odot}$ pc^{-2}), while B does the same for the thin disc (54 $M_{\odot}$ pc^{-2}) at the solar ring (Molero et al. 2023). Here, the θ function is the Heavyside step function.

2.5. Element production and chemical yields

It is worth reiterating that different elements are produced in different stars:

- Brown dwarfs with masses of <0.1 $M_{\odot}$ do not ignite H, and so they do not contribute to the chemical enrichment of the ISM, but they affect the chemical evolution by locking up gas.
- Very small stars in the mass range of 0.1 $M_{\odot}$–0.8 $M_{\odot}$ burn only H. They die as He WDs on timescales longer than the age of the Universe.
- Low- and intermediate-mass stars (LIMS) in the mass range 0.8–8.0 $M_{\odot}$ contribute to the chemical enrichment through post-MS mass loss and the final ejection of a planetary nebula. They produce mainly ^{4}He, CNO isotopes and heavy ($A > 90$) *s*-process elements.
- WDs in binary systems can give rise to Type Ia SNe or novae. Type Ia SNe are responsible for producing the bulk of Fe ($\simeq$0.60 $M_{\odot}$ per event) and enrich the medium with tracers of elements from C to Si. They also contribute other elements, such as C, Ne, Ca, and Mg, but in much smaller amounts compared to CC-SNe. Novae can be important producers of CNO isotopes and ^{7}Li.
- Massive stars from 8 to 10 $M_{\odot}$ burn O explosively (e-capture SNe). They produce mainly He, C, and O, and leave neutron stars as remnants.
- Massive stars in the mass range 10 $M_{\odot}$–M_{WR} end their lives as Type II SNe and explode by core collapse. The explosion leads to the formation of a neutron star or a black hole, depending on the amount of mass lost during their lives and the amount of ejected material that falls back on the contracting core. M_{WR} is the minimum mass for the formation of a Wolf-Rayet star. Its value depends on the stellar mass loss, which in turn depends on the progenitor characteristics in terms of initial mass and metallicity. For a solar chemical composition, $M_{WR} \simeq 25$ $M_{\odot}$. Stars with masses above M_{WR} end up as Type Ib/c and also explode by core collapse. They are linked to the long gamma-ray bursts (LGRBs) and can be particularly energetic, which has led to them being named hypernovae (HNe, Paczyński 1998). Massive stars are responsible for the production of most of α-elements (such as O, Ne, Mg, Si, S, and Ca), some Fe-peak elements, and light (A<90) *s*-process elements (especially if stellar rotation is included), and may also contribute to *r*-process nucleosynthesis (if strong magnetic field and fast rotation are included).
- Mergers of compact objects and in particular neutron stars and black hole binary systems can be powerful sources of *r*-process material.

The stellar yields that we adopt for stars of all masses, Type Ia SNe, and merging neutron stars are similar to those adopted in Romano et al. (2010) and Molero et al. (2023). In particular, for massive stars, we adopt the yields of Kobayashi et al. (2006) and the Geneva group (Meynet & Maeder 2002; Hirschi 2005, 2007; Ekström et al. 2008) for what concerns the CNO elements. For LIMS yields, we assume those of Karakas (2010), for Type Ia SNe those of Iwamoto et al. (1999), and for merging neutron stars as well as for massive stars dying as magneto-rotational SNe we adopt the same yields as those adopted by Molero et al. (2023) for neutron capture elements.

3. Results

3.1. The star formation rate

Before presenting the analysis of the abundance patterns, it is important to compare the evolution of the SFR predicted by our model at R_{GC}=8 kpc to present-day observations in the solar vicinity. The SFR, expressed in units of $M_{\odot}$ pc^{-2} Gyr^{-1}, is shown in Fig. 1. The gap between the two different disc phases, as discussed before, is clearly visible and the present-day value predicted by our model appears to be in close agreement with

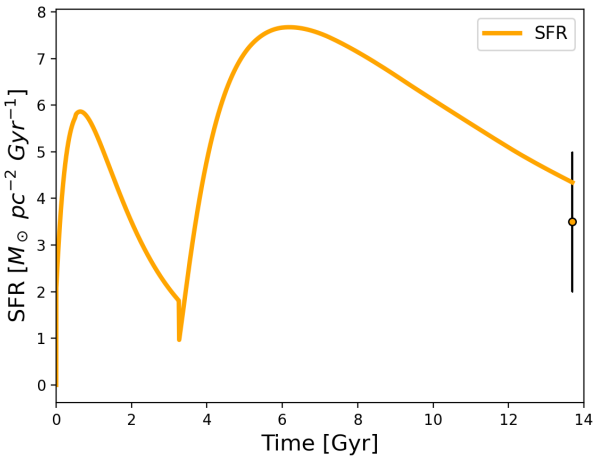

Fig. 1. Evolution with time of the SFR as predicted by the two-infall model for the solar vicinity. Observed present-day value is from Prantzos et al. (2018).

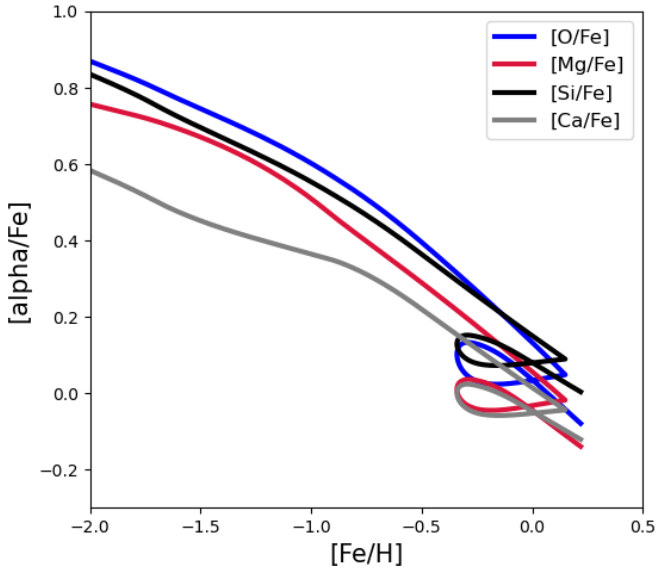

Fig. 2. [α/Fe] versus [Fe/H] abundance ratios predicted by our fiducial chemical evolution model for different α-elements in the solar vicinity: oxygen (blue line), magnesium (red line), silicon (black line), and calcium (grey line).

the measured value in the solar neighborhood, as suggested by Prantzos et al. (2018).

To compute how many solar masses of stars were formed up until the moment of the formation of the Solar System, we computed the integral of the SFR in the time interval 0.0–9.2 Gyr, as

$$\int_{0.0}^{9.2\,\mathrm{Gyr}} \psi(t)\,\mathrm{d}t = 51\ M_\odot \mathrm{pc}^{-2}. \quad (6)$$

This value, once multiplied by the area of the solar annular ring, which has a diameter of 2 kpc ($\sim 10^8$ pc^2), gives the total mass of all stars ever formed therein, which is equal to 5.1×10^9 M$_\odot$. We stress that this quantity also takes into account the contribution from the stellar remnants (namely WDs, neutron stars, and black holes).

For what concerns the total metallicity in the ISM 4.6 Gyr ago, we predict $Z_\odot$=0.0130, which is in excellent agreement with the solar metallicity by Asplund et al. (2009, $Z_\odot$=0.0134), and the predicted Fe abundance is 12 + log(Fe/H)$_\odot$=7.48, again in excellent agreement with the observed abundance.

3.2. Analysis of the [α/Fe] versus [Fe/H] plot by means of the time-delay model

In this section we present and analyse the [α/Fe] versus [Fe/H] abundance patterns We remind that the notation [X/Y] has the meaning [X/Y]= log(X/Y)−log(X/Y)$_\odot$ with X (Y) being the abundance by number of the element X (Y). of some α-elements, namely O, Mg, Si, and Ca. Figure 2 shows the plots of [α/Fe] versus [Fe/H] (α =O, Mg, Si, Ca) as predicted by the model. The time-delay model (Tinsley 1979; Matteucci 2012) provides a satisfying explanation for these paths: the ratio of [α/Fe] at very low metallicity is rather flat and (the slope of the 'flat' portion is due to the different nucleosynthetic yields of different α-elements).

Because only CC-SNe produce α elements in a substantial way plus some amount of Fe, the flat part of the plot is representative only of the contribution to the [α/Fe] ratio from massive stars at early times. When [Fe/H] ≥ -1.0 dex, Type Ia SNe start giving their contribution, as can be seen from the change of the slope shown in the plots. As mentioned above, this happens because Type Ia SNe are the main producers of Fe and eject this element into the ISM on longer timescales. The loop shown by the curves in Fig. 2 is due to the gap in the star formation occurring in between the two infall events. In fact, as explained in Spitoni et al. (2019), the second infall causes a dilution of the absolute abundances, producing a horizontal behavior in the [Fe/H] at almost constant [α/Fe]. Then, when the star formation recovers, the [α/Fe] ratio rises and then decreases slowly again because of the advent of Type Ia SNe. These loops can successfully explain the bimodality in [α/Fe] ratios (Spitoni et al. 2019, 2020).

If the X-axis can in principle be interpreted as a time axis, the [α/Fe] versus [Fe/H] relation can be used to extract the timescale for the formation of the thick and thin discs, knowing that thick disc stars have metallicities of ≤ -0.6 dex. Originally, Matteucci & Greggio (1986) derived the timescale of the formation of the inner-halo thick disc to be around 1.0–1.5 Gyr. Subsequent studies dealing with the detailed evolution of the thick disc confirmed a timescale of $\sim$1 Gyr for its formation (e.g. Micali et al. 2013; Grisoni et al. 2017). Here, we find the same timescale. It is worth noting that the timescale of formation of the thin disc at the solar ring is provided by the fit to the G-dwarf metallicity distribution and is $\sim$7 Gyr (e.g. Chiappini et al. 1997; Grisoni et al. 2017).

3.3. Rates and numbers of supernovae, white dwarfs, novae, merging neutron stars, and black holes

As the adopted chemical evolution model reproduces the solar metallicity and the abundance patterns in the solar vicinity quite well, now we can proceed to compute the rates and numbers of SNe (Type Ia and core-collapse), WDs, novae, neutron stars, and black holes that occurred until the formation of the Solar System in detail. Unless stating otherwise, we define the solar vicinity as the annular region centred on the Sun, as above, while for the whole disc we assume an area of approximately 10^9 pc^2.

3.3.1. Type Ia supernovae

To compute the number of Type Ia SNe that exploded up until the formation of the Solar System, we proceed in the same way as

for the total number of stars formed (see the previous section). In particular, we compute their rate as the fraction of WDs in binary systems that have the necessary conditions to give rise to a Type Ia SN event. This allows us to compute the rate of Type Ia SNe as suggested by Greggio (2005):

$$(Rate)_{SNeIa}(t) = K_\alpha \int_{\tau_i}^{min(t,\tau_x)} A(t-\tau)\psi(t-\tau)DTD(\tau)\,\mathrm{d}\tau, \quad (7)$$

where τ is the total delay time, namely the nuclear stellar lifetime of the secondary component of the binary system plus a possible delay due to the gravitational time delay in the DD model. $A(t-\tau)$ is the fraction of binary systems that give rise to SNe Type Ia and we assume it to be constant in time. The DTD(τ) is the delay time distribution function, which describes the rate of explosion of Type Ia SNe for a single starburst. The DTD is normalised as

$$\int_{\tau_i}^{\tau_x} DTD(\tau)\,\mathrm{d}\tau = 1, \quad (8)$$

with τ_i being the lifetime of a ~8 $M_\odot$ star and τ_x the maximum time for the explosion of a Type Ia SN. Here, we adopt the DTD for the wide DD scenario as suggested by Greggio (2005), where a detailed description can be found (see also Simonetti et al. 2019; Molero et al. 2021). Finally, K_α is a function of the IMF, namely

$$K_\alpha = \int_{0.1\ M_\odot}^{100\ M_\odot} \varphi(m)\,\mathrm{d}m. \quad (9)$$

The predicted present-time Type Ia SN rate for the whole disc is

$$(Rate)_{SNeIa,\,current} = 0.40 \cdot events/century. \quad (10)$$

It is important to notice that this result is in agreement with the observed rate of 0.43 events/century (Cappellaro & Turatto 1997; Li et al. 2011), which confirms the validity of the model.

We then compute the number of Type Ia SNe that took place in the solar vicinity until the birth of the Solar System. To do so, we integrate the rate from 0 Gyr to 9.2 Gyr, obtaining

$$N_{SNeIa}(t) = \int_0^{9.2\,Gyr} (Rate)_{SNeIa}(t)\,\mathrm{d}t = 2.87 \cdot 10^6. \quad (11)$$

3.3.2. Core-collapse supernovae

We compute the fraction of massive stars that will die as CC-SNe by assuming that they originate from single massive stars or massive binaries. The rate of Type II SNe is computed as

$$(Rate)_{SNeII}(t) = \int_{8\ M_\odot}^{M_{WR}} \psi(t-\tau_m)\varphi(m)\,\mathrm{d}m, \quad (12)$$

where, as previously described, M_{WR} is the limiting mass for the formation of a Wolf-Rayet star. The rate of Type Ib/Ic SNe can be calculated as (see Bissaldi et al. 2007):

$$(Rate)_{SNeIb,c}(t) = (1-\gamma)\int_{M_{WR}}^{M_{max}} \psi(t-\tau_m)\phi(m)\,\mathrm{d}m + \gamma \int_{14.8\ M_\odot}^{45\ M_\odot} \psi(t-\tau_m)\phi(m)\,\mathrm{d}m, \quad (13)$$

where the parameter γ is chosen to reproduce the number of massive binary systems in the range 14.8 ÷ 45 $M_\odot$ as proposed by Yoon et al. (2010) to produce a SNeIb,c. The mass M_{max} is the maximum mass allowed by the IMF, and is equal to 100 $M_\odot$.

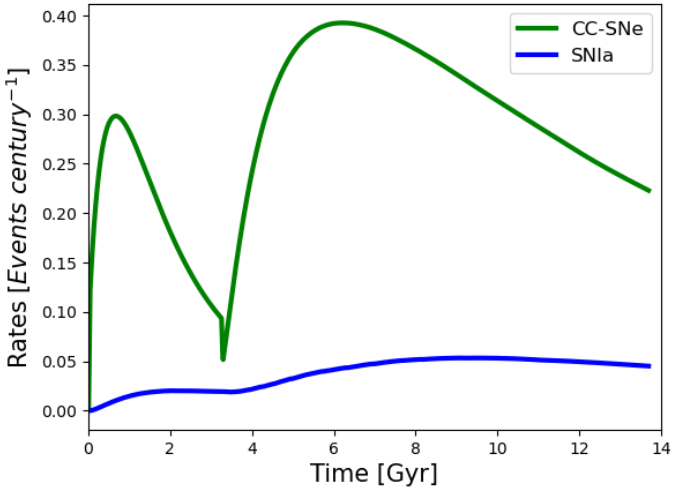

Fig. 3. Predicted rate of core-collapse (green line) compared to that of Type Ia SNe (blue line) in the solar vicinity.

Considering both SNeII and SNeIb,c, we obtain a total rate of CC-SNe of $(Rate)_{CCSNe,\,current}$=2.23 events/century, which is in agreement with rate calculated from observations, of namely 1.93 events/century (Cappellaro & Turatto 1997), as shown in Table 1. The total number of CC-SNe that exploded in the solar vicinity up until the formation of the Solar System is

$$N_{CCSNe}(t) = \int_0^{9.2\,Gyr} (Rate)_{CCSNe}(t)\,\mathrm{d}t = 26.47 \cdot 10^6. \quad (14)$$

In Fig. 3 we can see the CC-SN rate behaviour and appreciate the fact that, as expected, it follows the SFR path, namely it shows the same gap as the SFR versus time. Moreover, all the quantities related to the SFR, such as the CC-SN rate, the formation rate of neutron stars, and the black hole rates show a dip corresponding to the strong decrease in star formation occurring between the formation of the thick and thin discs. In the same figure, we show the Type Ia SN rate in the solar vicinity as a function of time. In Table 1, we finally summarise our results compared to observational data. It is worth noting that the observed current rates of SNe, as well as those of novae and MNSs, are derived for the entire MW, while we show in the figures the predicted rates for the solar ring. The predictions shown in Table 1, as well as in the other tables, refer instead to the entire disc, and, as it can be seen, the agreement between our predictions and data is quite good. Concerning the observed current rates for the solar vicinity, we could perhaps rescale those for the entire disc to the area of the solar vicinity. This would simply mean dividing the disc rates by a factor of ten.

3.3.3. White dwarfs and novae

In Fig. 4 we plot the rate of formation of WDs originating in the mass ranges 0.8–8 $M_\odot$, from which we obtain the number of WDs that formed in the solar vicinity until the moment of formation of the Solar System. This is computed as

$$N_{WD}(t) = \int_0^{9.2\,Gyr} (Rate)_{WD}(t)\,\mathrm{d}t = 423.88 \cdot 10^6. \quad (15)$$

Table 1. Comparison between observational data relative to SN rates (Cappellaro & Turatto 1997) compared with model results.

	Observational data (whole disc, present-day)	Rates (whole disc, present-day)	Numbers (solar vicinity, 9.2 Gyr of evolution)
SNeIa	0.43 SNe/century	0.45 SNe/century	2.87 million
CC-SNe	1.93 SNe/century	2.23 SNe/century	26.47 million

Notes. We can see that all theoretical values are consistent with observational data. In the first column, there are the observed rates, in the second column the predicted ones, and in the third column are the computed total numbers of SNe exploded from the beginning up to the formation of the Solar System.

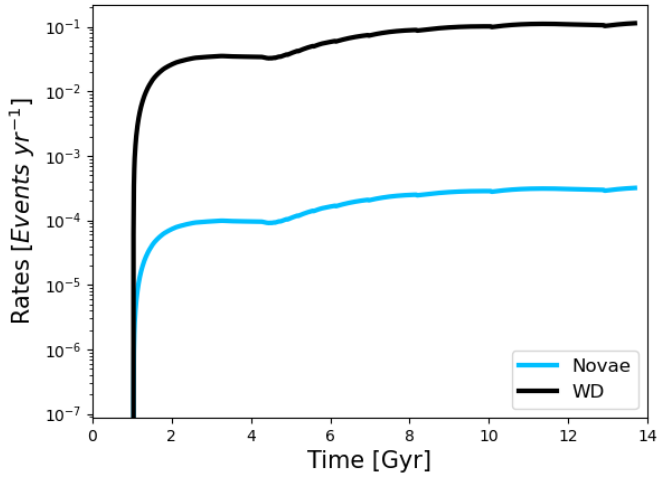

Fig. 4. Comparison of the rate of formation of nova systems and white dwarfs in the solar vicinity.

A nova outburst is caused by the thermonuclear runaway on top of a WD accreting H-rich matter from a close companion (a main sequence or a giant star) that overfills its Roche lobe. The system survives the explosion and the cycle is repeated approximately 10^4 times.

We compute the nova rate by assuming that it is a fraction of the WD rate. To do so, it is appropriate to define the parameter, $\alpha_{nova} < 1$, which represents the fraction of WDs that will form novae and is tuned to reproduce the present nova rate in the Galaxy. In this work, the value used is α_{nova}=0.0028 and this allows us to correctly reproduce the observed nova rate in the Galaxy, which is 20 ÷ 40 events/yr (Della Valle & Izzo 2020). Indeed, our model prediction is $(Rate)_{Novae,\,current} = 31$ number/yr. There are various ways to compute the rate of novae in our Galaxy, such as using the known novae to extrapolate for those too far to be seen, or observing novae in another galaxy and extrapolating their rate to the MW by assuming that every nova from the other galaxy can be seen.

In particular, we define the rate of novae as

$$(Rate)_{Novae}(t) = \alpha_{nova} \int_{0.8\ M_\odot}^{8\ M_\odot} \psi(t - \tau_{m_2} - \Delta t)\varphi(m)\,\mathrm{d}m, \tag{16}$$

with Δt being the delay time between the formation of the WD and the first nova outburst (the WD needs to cool down before the nova outburst can occur) and τ_{m_2} the lifetime of the secondary star that determines the start of the mass accretion onto the WD.

We had to consider that every nova system produces 10^4 nova outbursts, and so if we want to compute the nova rate, we need to multiply the nova formation rate by this number. In Fig. 4 we show the rates of WDs and novae together as functions of time. Table 2 shows the total rates and total numbers of WDs, novae, and nova outbursts.

The number of nova systems and nova outbursts that occurred in the solar vicinity until the moment of the formation of the Solar System is computed as

$$N_{Novae}(t) = \int_0^{9.2\,Gyr} (Rate)_{Novae}(t)\,\mathrm{d}t = 1.18 \cdot 10^6, \tag{17}$$

which leads us to the following result for the number of nova outbursts:

$$N_{NO}(t) = \int_0^{9.2\,Gyr} (Rate)_{NO}(t)\,\mathrm{d}t = 1.18 \cdot 10^{10}. \tag{18}$$

The numbers and rates of WDs and novae are presented in Table 2.

3.3.4. Neutron stars

Neutron stars are among the densest objects known, with an average density of around 10^{14} g/cm^3. They are remnants of massive stars, but the upper mass limit for the formation of a neutron star is unknown. In fact, if the stellar core is larger than the so-called Oppenheimer-Volkoff mass (~2 $M_\odot$), then a black hole will form. The limiting initial stellar mass between the formation of a neutron star and a black hole is strongly dependent on the assumptions in stellar models, such as the rate of mass loss during the evolution of massive stars. In the model adopted here to compute the rate of neutron stars, we assume that stars with masses from 9 to 50 $M_\odot$ (Molero et al. 2023) leave a neutron star after their death. With this assumption, we find that the current rate of formation of neutron stars is $(Rate)_{NS,\,current} \simeq 2.93 \times 10^4$ number/Myr.

3.3.5. Merging neutron stars

Merging neutron stars are important for what concerns the chemical evolution of galaxies, as they produce *r*-process elements. It was confirmed by the gravitational event GW170717 (Abbott et al. 2017) that the merger of neutron stars can produce a strong gravitational wave and that their contribution to the chemical composition of galaxies cannot be ignored. The rate of MNSs and their number are assumed to be proportional to the rate of formation of neutron stars (as proposed by Matteucci et al. 2014), namely

$$(Rate)_{MNS}(t) = \alpha_{NS} \cdot (Rate)_{NS}. \tag{19}$$

The constant α_{NS} is set to ~10^{-3}, and was chosen to correctly reproduce the observational rate of $83^{+209.1}_{-66.1}$ MNS/Myr

Table 2. Comparison between observational data about nova outbursts (Della Valle & Izzo 2020) and model results.

	Observational data (whole disc, present-day)	Rates (whole disc, present-day)	Numbers (solar vicinity, 9.2 Gyr of evolution)
Nova systems	–	0.0031 events/yr	1.18 million
Nova outbursts	25–30 events/yr	31 events/yr	11.8 billion
White dwarfs	–	1.11 events/yr	423 million

Notes. Theoretical rates of formation of WDs and nova systems are also reported, though observed rates of formation of WDs and nova systems are not available. The legend for Table 1 applies here also.

Table 3. Comparison between observational data relative to the MNS rate in the MW (Kalogera et al. 2004) and model results for neutron star and MNS formation rates.

	Observational data (whole disc, present-day)	Rates (whole disc, present-day)	Numbers (solar vicinity, 9.2 Gyr of evolution)
Neutron stars	–	29261 events/Myr	23.15 million
MNS	$83^{+209.1}_{-66.1}$ events/Myr	146 events/Myr	0.11 million

Notes. We can see that the computed value for the MNS rate is consistent with observational data and results by Molero et al. (2021). We note that these values were obtained with $\alpha_{NS} = 0.005$.

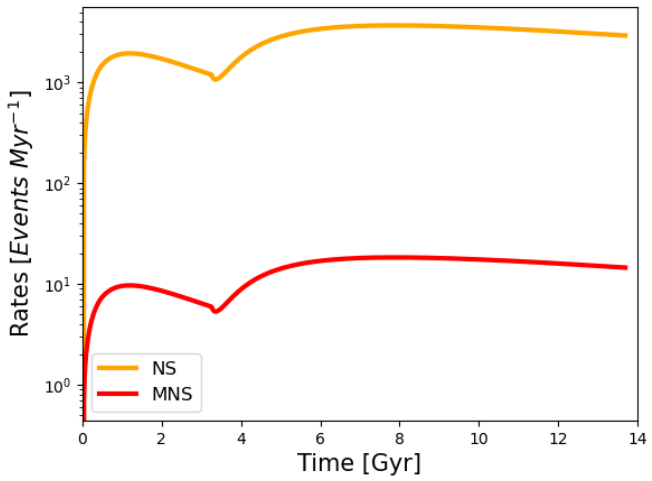

Fig. 5. Rates of neutron star (yellow line) and MNS formation (red line) predicted by our chemical evolution model for the solar vicinity.

(Kalogera et al. 2004) in the MW. Finally, the total numbers of neutron stars and MNSs in the solar vicinity that contributed to the chemical composition of the Solar System were obtained as the time integral of their rates, namely

$$N_{NS}(t) = \int_0^{9.2\,Gyr} (Rate)_{NS}(t)\,\mathrm{d}t = 23.15 \cdot 10^6, \tag{20}$$

and

$$N_{MNS}(t) = \int_0^{9.2\,Gyr} (Rate)_{MNS}(t)\,\mathrm{d}t = 0.11 \cdot 10^6. \tag{21}$$

A plot with both neutron star and MNS rates is provided in Fig. 5. The numbers and rates of neutron stars and MNSs can be found in Table 3.

3.3.6. Black holes

The last rate that we computed is the rate of birth of black holes originating from the massive stars that can leave a black hole after their death. The rate of formation of black holes is

$$(Rate)_{BH}(t) = \int_{M_{BH}}^{100\ M_\odot} \psi(t)\varphi(m)\,\mathrm{d}m. \tag{22}$$

In our model, we assume two different values of M_{BH} (the limiting initial stellar mass for having a black hole as a remnant), namely M_{BH}=30 $M_\odot$ and M_{BH}=50 $M_\odot$. The total number of black holes that formed in the solar vicinity until the formation of the Solar System is computed as

$$N_{BH} = \int_0^{9.2\,Gyr} (Rate)_{BH}(t)\,\mathrm{d}t. \tag{23}$$

The first choice, M_{BH}=30 $M_\odot$, led us to the result that roughly 9.14% of massive stars will leave a black hole, which means $N_{BH} \sim 2.46 \cdot 10^6$, while for M_{BH}=50 $M_\odot$ the number drops to 3.00%, that is $N_{BH} \sim 0.82 \cdot 10^6$ (see Table 4). Figure 6 provides a comparison between the rate of black holes under the assumptions of $M_{BH} \geq 30$ $M_\odot$ and $M_{BH} \geq 50$ $M_\odot$, as well as the rate of CC-SNe.

3.3.7. Comparison of all the rates

To obtain a complete picture of all the types of stars that contributed to the formation of the Solar System and to its chemical composition, it is interesting to plot the different rates together, so that it is possible to better compare them.

In particular, in Fig. 7 we report all the rates discussed up to now together for comparison. It is clear from the figure that the nova outbursts, for the assumptions made, represent the largest number of events, but the material ejected during each burst is much less than what is produced by SNe and MNSs. However, novae cannot be neglected in chemical evolution models, as they can be responsible for the production of some important species. We underline that black holes (M_{BH}=30 $M_\odot$) are represented in this graph despite the fact that they do not contribute

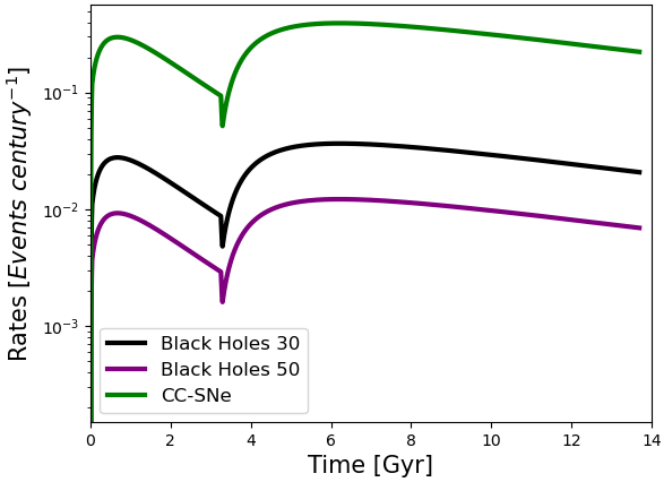

Fig. 6. Comparison between the rate of black holes that come from stars with masses of ≥30 $M_\odot$ (black line) and from stars with masses of ≥50 $M_\odot$ (purple line) with CC-SNe (green line), in the solar vicinity.

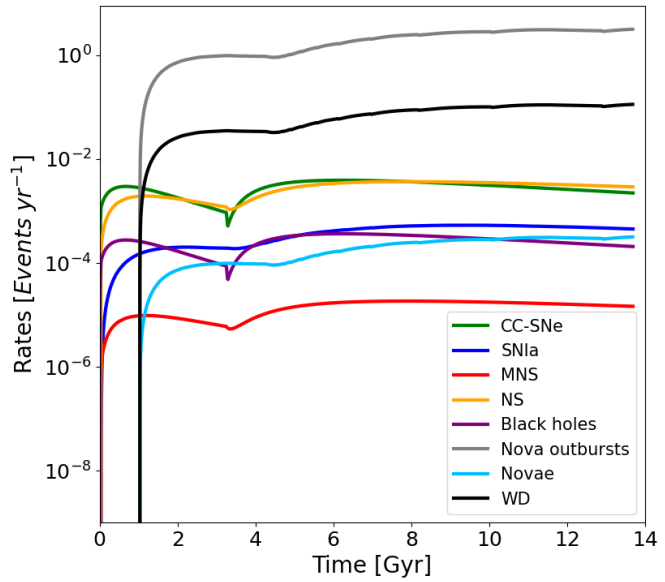

Fig. 7. Rates of all types of stars in the solar vicinity, as discussed up until now. We note that some types of stars, namely WDs, novae, and nova outbursts, started forming after t ∼ 1 Gyr and not immediately following the Big Bang.

to the chemical enrichment. This is because they are related to very massive stars that can eject large amounts of metals before dying. Moreover, stars leaving black holes as remnants (Type Ib and Ic SNe) seem to be related to long GRBs, and the rate of formation of black holes can therefore trace the rate of these events (see Bissaldi et al. 2007).

In Fig. 8 we show a stellar pie chart illustrating the different percentages of stellar contributors to the chemical composition of the Solar System. Clearly, the majority of stars ever born and dead from the beginning to the formation of the Solar System belong to the range of low and intermediate masses; these stars mainly contributed to the production of He, with some contributing C, N, and heavy *s*-process elements, while the massive stars whose remnants are neutron stars and black holes, produced the majority of the α-elements, in particular O, which dominates the total solar metallicity Z. On the other hand, the majority of the Fe originates from Type Ia SNe. The novae can be important producers of CNO isotopes (see Romano 2022) and perhaps ^{7}Li (see Izzo et al. 2015; Cescutti & Molaro 2019; Matteucci et al. 2021). Concerning *r*-process elements, the most reasonable assumption is that they were produced by stars in the range of massive stars, both MNSs and some peculiar types of CC-SNe (see Simonetti et al. 2019; Molero et al. 2023).

Table 4. Comparison between different model results concerning the number of black holes with $M_{BH} \geq 30\ M_\odot$ and $M_{BH} \geq 50\ M_\odot$ as a percentage of massive stars.

Black holes	$M_{BH} \geq 30\ M_\odot$	$M_{BH} \geq 50\ M_\odot$
Percentage	9.14%	3.00%
Number	2.46 million	0.82 million

4. The number of stars similar to the Sun born from the beginning up to the formation of the Solar System

In order to investigate a crucial aspect of the general argument of the evolution of the Galactic population of stars and their habitable planets, let us introduce the concept of the number of solar twins born before our Sun. Although it is known that M stars (0.08–0.45 $M_\odot$) can also host Earth-like planets, and the number of these stars has been computed for the MW (see Spitoni et al. 2017), here we focus on (life bearing) twins of our Sun as hosts of Earth-like planets. Hence, we compute the number of stars in the range of mass of 0.92–1.08 $M_\odot$ born from the Big Bang up to 4.6 ±0.1 Gyr ago and with solar Fe abundance compatible (within 1σ) with the value from Asplund et al. (2009), who reported 7.50 ± 0.04 dex. In other words, this quantity, $N_\odot$, is the number of solar twins formed in the vicinity of the current location of the Sun until 4.6 Gyr ago. Such a time limit is set because we take the working assumption that, on average, intelligent life would develop in the twin solar systems within the same time as was required on Earth. We then obtain $N_\odot \simeq 31.70 \times 10^6$. Among $N_\odot$, our Sun is the $\sim 2.61 \cdot 10^7$-th star born in the solar vicinity with a predicted Fe abundance of 7.48 dex, in excellent agreement with the observed one.

Figure 9 shows the Fe abundance in terms of mass as a function of Galactic age, as predicted for the solar vicinity. The peak of the Fe abundance at early times corresponds to the formation of the thick disc; a gap then follows due to the strong depression of the SFR between the formation of the thick and thin discs, and finally an increase of the Fe abundance up to the time of formation of the Solar System and beyond. Additionally, the figure shows the cumulative number of stars with the same mass and Fe abundance formed up to the appearance of our Sun. Notably, at early times, during the age interval from 11.12 Gyr to 10.36 Gyr ago, a total of $\sim 0.77 \times 10^7$ solar-like stars were already formed. Then, due to the strong metallicity dilution by the infalling gas with a pristine chemical composition associated with the formation of the thin disc, the Fe abundance decreased and remained subsolar until 4.91 Gyr ago. In more recent times, that is, during Galactic ages of between 4.91 and 4.50 Gyr, $\sim 2.40 \times 10^7$ Suns were formed (∼75.6% of the total number).

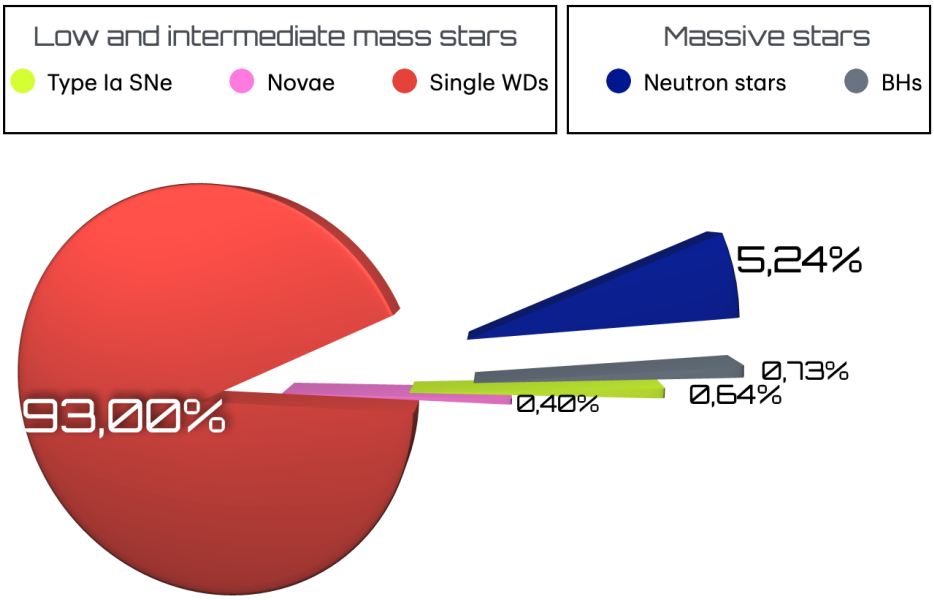

Fig. 8. Percentage contributions made by the stars analysed in this paper (identified with their final outcomes) to the chemical composition of the Solar System.

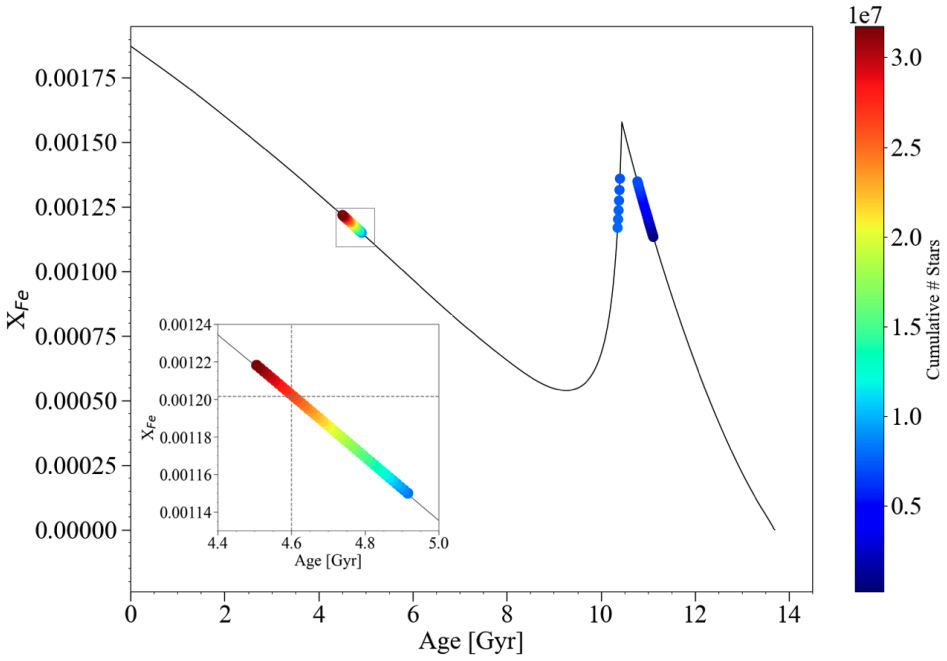

Fig. 9. Iron mass fraction X_{Fe} versus Galactic age, obtained with our chemical evolution model for the solar vicinity. With the colour-coded points, we highlight the cumulative number of stars that share the same physical and chemical properties of our Sun formed from the beginning up to 4.6 ± 0.1 Gyr ago (see Sect. 4 for further details). In the inset plot we zoom in on the region with predicted Sun-like stars younger than 4.91 Gyr. The horizontal dashed line indicates the iron mass fraction predicted for our Sun born 4.6 Gyr ago (vertical dashed line).

5. Conclusions and discussion

In this work, we calculated the rates and the relative numbers of stars of different masses that died either quiescently or in an explosive way as SNe and thus contributed to the chemical composition of the Solar System (which formed about 4.6 Gyr ago) in the context of the two-infall model for the chemical evolution of the Milky Way.

We calculated the following numbers for each type of star residing in the solar vicinity:

- Type Ia supernovae: 2.87 million
- Core-collapse supernovae: 26.47 million
- White dwarfs: 423.88 million
- Nova systems: 1.8 million
- Nova outbursts: $1.8 \cdot 10^4$ million
- Neutron stars: 23.5 million
- Merging neutron stars: 0.11 million
- Black holes ($M \geq 30\ M_\odot$): 2.46 million
- Black holes ($M \geq 50\ M_\odot$): 0.82 million
- Solar twins born 4.6 Gyr ago: 31 million
- Stars ever born and still alive 4.6 Gyr ago: 3.5 billion.

It is worth noting that all these numbers should be divided by 25 if restricting the solar vicinity area to a square centred on the Sun with a side of 2 kpc. Concerning the percentage of black holes that formed up until the birth of the Solar System in relation to the number of massive stars ($8\ M_\odot \leq M \leq 100\ M_\odot$), we find that only 3% of massive stars have the necessary characteristics to become black holes if we assume a limiting mass for the formation of black holes of $\geq 50\ M_\odot$, while the percentage increases to 9% if we accept stars with $M \geq 30\ M_\odot$.

Finally, since our aim is to understand how different types of stars contributed to the chemical composition of the solar neighbourhood, in particular its metallicity, we estimated the percentages of the contributions of different types of stars to

the α−elements and Fe, which are the major constituents of the metallicity Z. In particular, ^{16}O is almost entirely (98.5%) produced by stars with masses of $>8\,M_{\odot}$, as is ^{24}Mg (98.2%). For the other α-elements, Ca and Si, we find that 74.5% and 79%, respectively, is produced by massive stars, with the rest being produced by Type Ia SNe. Finally, we find 70% of Fe to be produced by Type Ia SNe, with the remaining 30% coming from massive stars, in agreement with a previous calculation (Matteucci & Greggio 1986). It is worth noting that these percentages depend on the assumed stellar yields and IMF. However, as both yields and IMF are suitable for the solar vicinity, we are confident that the percentages are correct.

Acknowledgements. F.M., M.M. and A.V. thank I.N.A.F. for the 1.05.12.06.05 Theory Grant - Galactic archaeology with radioactive and stable nuclei. F. Matteucci also thanks Ken Croswell for stimulating the computation of the total number of novae, thus giving the idea for the present paper. This research was supported by the Munich Institute for Astro-, Particle and BioPhysics (MIAPbP) which is funded by the Deutsche Forschungsgemeinschaft (DFG, German Research Foundation) under Germany´s Excellence Strategy – EXC-2094 – 390783311. F.M. thanks also support from Project PRIN MUR 2022 (code 2022ARWP9C) "Early Formation and Evolution of Bulge and HalO (EFEBHO)" (PI: M. Marconi), funded by the European Union – Next Generation EU. E. Spitoni thanks I.N.A.F. for the 1.05.23.01.09 Large Grant - Beyond metallicity: Exploiting the full POtential of CHemical elements (EPOCH) (ref. Laura Magrini). This work was supported by the Deutsche Forschungsgemeinschaft (DFG, German Research Foundation) – Project-ID 279384907 – SFB 1245, the State of Hessen within the Research Cluster ELEMENTS (Project ID 500/10.006). Finally, we thank an anonymous referee for very useful suggestions that improved the paper.

References

Abbott, B. P., Abbott, R., Abbott, T. D., et al. 2017, Phys. Rev. Lett., 119, 161101
Asplund, M., Grevesse, N., Sauval, A. J., & Scott, P. 2009, ARA&A, 47, 481
Bissaldi, E., Calura, F., Matteucci, F., Longo, F., & Barbiellini, G. 2007, A&A, 471, 585
Bouvier, A., & Wadhwa, M. 2010, Nat. Geosci., 3, 637
Cappellaro, E., & Turatto, M. 1997, ASI Ser. C, 486, 77
Cescutti, G., & Molaro, P. 2019, MNRAS, 482, 4372
Chiappini, C., Matteucci, F., & Gratton, R. 1997, ApJ, 477, 765
Chiappini, C., Matteucci, F., & Romano, D. 2001, ApJ, 554, 1044
Della Valle, M., & Izzo, L. 2020, A&A Rev., 28, 3
Ekström, S., Meynet, G., Chiappini, C., Hirschi, R., & Maeder, A. 2008, A&A, 489, 685
Fuhrmann, K. 1998, A&A, 338, 161
Gratton, R., Carretta, E., Matteucci, F., & Sneden, C. 1996, in ASP Conf. Ser., 92, 307
Greggio, L. 2005, A&A, 441, 1055
Grisoni, V., Spitoni, E., Matteucci, F., et al. 2017, MNRAS, 472, 3637
Hayden, M. R., Holtzman, J. A., Bovy, J., et al. 2014, AJ, 147, 116
Hayden, M. R., Bovy, J., Holtzman, J. A., et al. 2015, ApJ, 808, 132
Hirschi, R. 2005, IAU Symp., 228, 331
Hirschi, R. 2007, A&A, 461, 571
Iwamoto, K., Brachwitz, F., Nomoto, K., et al. 1999, ApJS, 125, 439
Izzo, L., Della Valle, M., Mason, E., et al. 2015, ApJ, 808, L14
Kalogera, V., Kim, C., Lorimer, D. R., et al. 2004, ApJ, 614, L137
Karakas, A. I. 2010, MNRAS, 403, 1413
Kawata, D., & Chiappini, C. 2016, Astron. Nachr., 337, 976
Kennicutt, Jr., R. C. 1998, ApJ, 498, 541
Kobayashi, C., Umeda, H., Nomoto, K., Tominaga, N., & Ohkubo, T. 2006, ApJ, 653, 1145
Kroupa, P., Tout, C. A., & Gilmore, G. 1993, MNRAS, 262, 545
Li, W., Chornock, R., Leaman, J., et al. 2011, MNRAS, 412, 1473
Matteucci, F. 2012, Chemical Evolution of Galaxies (Berlin: Springer)
Matteucci, F. 2021, A&A Rev., 29, 5
Matteucci, F., & Francois, P. 1989, MNRAS, 239, 885
Matteucci, F., & Greggio, L. 1986, A&A, 154, 279
Matteucci, F., Romano, D., Arcones, A., Korobkin, O., & Rosswog, S. 2014, MNRAS, 438, 2177
Matteucci, F., Molero, M., Aguado, D. S., & Romano, D. 2021, MNRAS, 505, 200
Melioli, C., Brighenti, F., D'Ercole, A., & de Gouveia Dal Pino, E. M. 2009, MNRAS, 399, 1089
Meynet, G., & Maeder, A. 2002, A&A, 390, 561
Micali, A., Matteucci, F., & Romano, D. 2013, MNRAS, 436, 1648
Mikolaitis, Š., de Laverny, P., Recio-Blanco, A., et al. 2017, A&A, 600, A22
Molero, M., Simonetti, P., Matteucci, F., & della Valle, M. 2021, MNRAS, 500, 1071
Molero, M., Magrini, L., Matteucci, F., et al. 2023, MNRAS, 523, 2974
Paczyński, B. 1998, ApJ, 494, L45
Palla, M., Matteucci, F., Spitoni, E., Vincenzo, F., & Grisoni, V. 2020, MNRAS, 498, 1710
Prantzos, N., Abia, C., Limongi, M., Chieffi, A., & Cristallo, S. 2018, MNRAS, 476, 3432
Recio-Blanco, A., de Laverny, P., Kordopatis, G., et al. 2014, A&A, 567, A5
Recio-Blanco, A., de Laverny, P., Palicio, P. A., et al. 2023, A&A, 674, A29
Romano, D. 2022, A&A Rev., 30, 7
Romano, D., Matteucci, F., Salucci, P., & Chiappini, C. 2000, ApJ, 539, 235
Romano, D., Chiappini, C., Matteucci, F., & Tosi, M. 2005, A&A, 430, 491
Romano, D., Karakas, A. I., Tosi, M., & Matteucci, F. 2010, A&A, 522, A32
Romano, D., Matteucci, F., Zhang, Z.-Y., Ivison, R. J., & Ventura, P. 2019, MNRAS, 490, 2838
Schmidt, M. 1959, ApJ, 129, 243
Simonetti, P., Matteucci, F., Greggio, L., & Cescutti, G. 2019, MNRAS, 486, 2896
Spitoni, E., Matteucci, F., Recchi, S., Cescutti, G., & Pipino, A. 2009, A&A, 504, 87
Spitoni, E., Gioannini, L., & Matteucci, F. 2017, A&A, 605, A38
Spitoni, E., Silva Aguirre, V., Matteucci, F., Calura, F., & Grisoni, V. 2019, A&A, 623, A60
Spitoni, E., Verma, K., Silva Aguirre, V., & Calura, F. 2020, A&A, 635, A58
Spitoni, E., Verma, K., Silva Aguirre, V., et al. 2021, A&A, 647, A73
Spitoni, E., Matteucci, F., Gratton, R., et al. 2024, A&A, 690, A208
Tinsley, B. M. 1979, ApJ, 229, 1046
Yoon, S. C., Woosley, S. E., & Langer, N. 2010, ApJ, 725, 940